The catabolism of alanine and glutamate ensure proper sporulation by preventing premature germination and providing energy sources respectively

Fengzhi Lyu[1], Tianyu Zhang[1], Dong Yang[1], Meng Gui[2], Yongtao Wang[1], Xiaojun Liao[1], Lei Rao[1]

[1] College of Food Science and Nutritional Engineering
National Engineering Research Center for Fruit and Vegetable Processing
Key Laboratory of Fruit and Vegetable Processing of Ministry of Agriculture and Rural Affairs
Beijing Key Laboratory for Food Non-Thermal Processing
China Agricultural University
Beijing, China

[2] Beijing Fisheries Research Institute
Beijing Academy of Agriculture and Forestry Sciences
Beijing, China

Correspondence
Lei Rao, College of Food Science and Nutritional Engineering, China Agricultural University, 100083, Beijing, China
Email: rao.lei@cau.edu.cn

ABSTRACT

Sporulation as a typical bacterial differentiation process has been studied for decades, and the morphological events along with the molecular regulation mechanisms are relatively clear. However, two other important aspects of sporulation, (i) how sporulating cells gain energy sources to fuel sporulation proceeding, and (ii) how generated spores maintain dormancy during the whole sporulation process lack research. Here, we found that RocG-mediated glutamate metabolism was crucial for driving mother cell lysis to succeed sporulation, likely by providing energy metabolites ATP. Interestingly, high-level rocG expression generated excessively high ATP contents in sporulating cells, which caused adverse effects on the properties of the future spores, e.g. faster germination efficiency, lower DPA content along with decreased heat resistance. Moreover, we revealed that Ald-mediated alanine metabolism decreased the typical germinant L-alanine concentration to a certain level in the sporulating environment, thus avoiding premature germination and maintaining spore dormancy. Our data inferred that sporulation was a highly orchestrated and exquisite biological process requiring the balance of diverse metabolism pathways, hence ensuring both the sporulation completion and the high quality of generated spores.

INTRODUCTION

Spores are formed by bacteria belonging to the orders *Bacillales* and *Clostridiales* in response to unfavorable environmental conditions such as nutrient limitation (1, 2). Spores are metabolically dormant and considered as the most resilient living organisms due to their extreme resistance to harsh environment and can exist for even millions of years (3-5). The process of forming spores from bacterial vegetative cells is termed sporulation. Taking the model bacterium *Bacillus subtilis* as an example, the morphological process of sporulation can be divided into several stages, including asymmetric division, engulfment, spore maturation, mother cell lysis and spore release (6). Specifically, as vegetative cells commit themselves to sporulation, the earliest visible event is the asymmetric division, producing the septum to divide the vegetative cell into a larger mother cell and a smaller forespore. Subsequently, the mother cell membrane migrates around the forespore until it is completely enclosed. This phagocytosis-like process is identified as engulfment. At this time, the double-membrane structure of forespore forms, followed by the cortex synthesis and spore coat assembly. Then, the forespore chromosomes are saturated with small acid-soluble proteins (SASPs), and the water in the forespore is replaced by DPA synthesized in the mother cell, leading to forespore dehydration. These events lead to the appearance of phase-bright spores. Next, mother cell lysis occurs after spore maturation, allowing the spores to be released into the environment.

Research on the morphological events of the sporulation process, as well as the underlying gene expression and molecular mechanisms, has been continued for decades (6-10). However, relative few research focuses on how to guarantee proper sporulation, especially the quantity and quality of spores. When referred to proper sporulation, we essentially indicate two aspects. The first one is the normal progression of the sporulation event. Since sporulation

is considered as an energy-consuming biological process (11), the energy supply is critical to promote the progress of the sporulation event. Studies have speculated that amino acid metabolism, such as glutamate and alanine metabolism, are potential energy sources that drive sporulation (12-14). However, their regulatory mechanisms during sporulation remain unclear. The second aspect is that the spores should remain dormant during the whole sporulating process. Although depletion of nutrients in the environment is a prerequisite for sporulation initiation (15), quantities of factors that induce germination still exist around generated spores. How the spores keep dormant in that tempting environment remains a mystery to be explored. Previous research has reported that the deletion of *ylbJ*, *pdaB*, or SpoVA protein encoding genes led to the loss of dormancy maintaining ability, as these mutants exhibited premature germination during sporulation (16, 17). The reasons for premature germination are diverse, including inappropriate activation of germination receptors, incorrect assembly of spore outer structure, and deficiency in the SpoVA channel. Hence, defects in any aspect will lead to abnormal sporulation and adversely affect the quantity or quality of spores produced. However, the precise mechanism of how spore maintain dormancy during sporulation is still unclear.

Here, we reported that the RocG-mediated glutamate metabolism played a crucial role in ensuring proper sporulation, especially promoting the mother cell lysis, by providing energy sources. We also found that high level *rocG* expression caused excessively high ATP contents in sporulating cells, which adversely affected the properties of the correspondingly generated spores, including faster germination efficiency, lower DPA content along with decreased heat resistance. Moreover, we also revealed that the Ald-mediated alanine metabolism decreased the concentration of the typical germinant L-alanine in sporulating environment to a certain level, thus avoiding premature germination and maintaining spore dormancy.

RESULTS

Proteins regulating alanine, aspartate and glutamate metabolism are enriched by proteomics analysis during sporulation of *B. subtilis*

In order to explore the metabolic pathways crucial for *B. subtilis* sporulation, Tandem Mass Tag-based (TMT) quantitative proteomics analysis was carried out between dormant spores (DS) and sporulating vegetative cells (VC) at t_0 (Figure 1A). Hierarchical clustering analysis (HCA) was conducted to exhibit the overall differences of protein expression between DS and VC group (Figure 1B). Greater differences between groups were showed in the HCA heatmap than that within groups, indicating that the protein expression in DS and VC was significantly different. The differentially-expressed proteins were screened with the criteria $p < 0.05$ and fold change > 1.2 (the expression level increased by more than 1.2-fold or decreased by less than 0.83-fold). 1,259 proteins with increased expression as well as 1,248 proteins with deceased expression were screened out in VC group (Figure 1C). KEGG pathway enrichment analysis of these differently expressed proteins revealed the great changes in several metabolism between DS and VC groups, including alanine, aspartate and glutamate metabolism, ribosome, flagellar assembly, glyoxylate and dicarboxylate metabolism, and methane metabolism (Figure 1D). Among these pathways, the most significant changes were identified in alanine, aspartate and glutamate metabolism, suggesting their crucial roles in the sporulation of *B. subtilis*. Previous studies have indicated that *ald*, encoding alanine dehydrogenase Ald, and *rocG*, encoding glutamate dehydrogenase RocG, are crucial regulators of alanine and glutamate metabolism, respectively (13, 18). In addition, Δ*ald* and Δ*rocG* mutants have been verified to exhibit remarkable sporulation deficiency (13, 14). However, the deletion of *ansB* gene, encoding L-aspartase important for aspartate metabolism, has no significant effect on sporulation (19). Hence, the effects of alanine and glutamate metabolism on

139 sporulation were further explored in this work.

140

141 **Alanine and glutamate metabolism co-regulate sporulation with an**
142 **additive effect**

143

144 Since alanine and glutamate metabolism have been reported separately to be
145 involved in sporulation (13, 14, 20), we wonder if these two pathways can jointly
146 affect the sporulation process. To verify this hypothesis, we constructed Δ*ald*
147 Δ*rocG* mutant and observed that significant fewer phase-bright spores were
148 produced in the double mutant strain than in Δ*ald* or Δ*rocG* mutants (Figure 2A).
149 This result indicated that the sporulation defect of Δ*ald* Δ*rocG* mutant was more
150 significant than that of Δ*ald* or Δ*rocG* mutants. This was further demonstrated
151 by examining the heat-resistant spores produced in sporulation, as the
152 percentage of Δ*ald* and Δ*rocG* spores was 10.9% and 29.8% respectively, while
153 Δ*ald* Δ*rocG* mutant was only 0.3% (Figure 2B). The severe sporulation
154 deficiency of Δ*ald* Δ*rocG* mutant suggested that Ald and RocG co-regulated
155 sporulation in an additive effect. Moreover, quantities of phase-dark forespores
156 were observed in Δ*ald* Δ*rocG* mutant (Figure 2A), which could be attributed to
157 two reasons including (i) limited energy sources supporting the sporulation
158 proceeding, or (ii) premature germination caused by abnormal spore structure
159 assembly or inappropriate in-situ sporulating environment (16). We then
160 deleted *gerAA* to investigate if premature germination occurred in Δ*ald* Δ*rocG*
161 mutant. As shown in Figure 3A, the sporulation defect of the double mutant was
162 partially rescued, as 29.7% of phase-bright spores formed in Δ*ald* Δ*rocG*
163 Δ*gerAA* (Δ3) mutant, indicating that premature germination indeed existed.
164 However, the only partial rescue effect suggested that premature germination
165 was not the exclusive reason of the sporulation defect in Δ*ald* Δ*rocG* mutant.
166 Hence, the limitation of energy support can still be a substantial explanation of
167 sporulation defect phenotype of the double mutant strain. We then explored
168 these two possibilities in the following work.

169 **RocG-mediated glutamate metabolism, but not Ald-mediated alanine**
170 **metabolism, is essential for ensuring the sporulation efficiency and the**
171 **spore quality likely through energy supply**
172
173 As the Ald and RocG mediated alanine and glutamate metabolisms were
174 proposed as potential energy sources for sporulation (13, 14), we speculated
175 that these two metabolic pathways provided energy support separately. If this
176 was the case, excessive complementation of either metabolism pathway should
177 be able to rescue the sporulation defect of the Δ*ald* Δ*rocG* mutant. Here, we
178 used Δ*ald* Δ*rocG* Δ*gerAA* (Δ3) strain to exclude the premature germination
179 effect and independently explored the energy supply mechanism in this part
180 (Figure 3A). Based on this, *ald* and *rocG* were artificially expressed separately
181 and jointly in Δ3 under IPTG-inducible promoter. Results showed that elevating
182 the expression level of *ald* by increasing the concentration of IPTG up to 5 mM
183 had no significant effect on the quantity of phase-bright spores in Δ3 mutant,
184 with the sporulation percentage between 20% and 30% (Figure S1, Figure S2A).
185 Accordingly, these spores showed significant germination deficiency under
186 AGFK induction (Figure S2B, Figure 3C). However, the elevated *rocG*
187 expression level upon addition of at least 10 mM IPTG restored the sporulation
188 of Δ3 mutant to 53.4%, similar with that of wild-type (56.8%) (Figure 3B).
189 Moreover, when more than 20 mM IPTG was added, the germination deficiency
190 of Δ3 mutant spores was recovered to the level of wild-type (Figure S2B, Figure
191 3C). Notably, Δ3 mutant with IPTG-induced *ald* and *rocG* co-expression
192 showed the same sporulation and germination phenotypes as that with IPTG-
193 induced *rocG* sole expression (Figure S2B, Figure 3C). Hence, in Δ3 mutant,
194 the sole complementation of RocG succeeded to rescue the sporulation defect,
195 but not the case for that of Ald. This indicated that RocG-mediated glutamate
196 metabolism appeared to regulate sporulation by providing energy sources
197 whereas Ald-mediated alanine metabolism may not play the same role.
198

199 To further explore if these two catabolism pathways are involved in controlling
200 the spore quality, mutants of transcription factors of Ald and RocG, Δ*adeR* and
201 Δ*ahrC* Δ*rocR* (14, 21), were respectively constructed to test the germination
202 phenotype of the spores. *gerAA* was also knocked out in these mutants to
203 ensure the comparability of experimental results. The deletion of transcription
204 factors was demonstrated to lower, instead of eliminating the expression of
205 regulated genes (Figure 4B), and rescued the sporulation deficiency (Figure
206 4A). Interestingly, no significant germination defect was observed in spores of
207 Δ*adeR* Δ*gerAA* mutant with decreased expression of *ald* (Figure 4C). However,
208 spores of Δ*ahrC* Δ*rocR* Δ*gerAA* mutant with low expression of *rocG* showed
209 remarkable germination deficiency (Figure 4C). Moreover, spores of Δ*adeR*
210 Δ*ahrC* Δ*rocR* Δ*gerAA* mutant exhibited similar germination deficiency
211 phenotype with that of Δ*ahrC* Δ*rocR* Δ*gerAA* mutant spores (Figure 4C),
212 indicating that the expression of *rocG*, not *ald*, was essential for ensuring spore
213 quality with normal germination capability. Taken together, these results
214 strongly implied that the RocG-mediated glutamate metabolism regulated both
215 the sporulation efficiency and spore quality likely by energy supply. As for the
216 Ald-mediated alanine metabolism, its effect on sporulation was not likely
217 executed by providing energy sources. Instead, it is more likely associated with
218 premature germination, as quantities of phase-dark spores were observed in
219 the sporulating cells of Δ*ald* mutant (Figure 2A).
220
221 **Ald inhibits premature germination during sporulation by regulating L-**
222 **alanine content in the external environment of spores**
223
224 As mentioned above, the occurrence of phase-dark spores in Δ*ald* mutant
225 drove us to investigate the effect of Ald-mediated alanine metabolism on
226 premature germination. As shown in Figure 5, Δ*ald* mutant generated large
227 amounts of phase-dark spores, and the percentage of phase-bright spores was
228 only 11.5%. However, the deletion of *gerAA* in Δ*ald* mutant significantly raised

229 the percentage of phase-bright spores to 61.5%, nearly close the wild type
230 (76.5%). In addition, no significant germination deficiency was observed in Δ*ald*
231 Δ*gerAA* spores when compared with wild-type (Figure 5C). Thus, it could
232 conclude that the absence of Ald caused sporulation defect by inducing
233 premature germination during sporulation. In order to identify the period of
234 premature germination occurrence, the sporulation process of Δ*ald* mutant was
235 examined by time-lapse microscopy. Interestingly, two models of premature
236 germination were observed as (i) forespores prematurely germinated during
237 mother cell lysis, and then released; (ii) dormant spores were released, and
238 then induced to premature germination (Figure 5D).
239
240 The association of Ald and premature germination raised up an interesting
241 speculation that the interruption of alanine metabolism may lead to the over-
242 accumulation of L-alanine, which triggers premature germination. To test this
243 possibility, *ald* was artificially expressed in Δ*ald* mutant under IPTG-inducible
244 promoter, and the sporulation phenotype as well as the environmental L-alanine
245 content at later sporulation phase (t_{19}) of these mutants were examined. Results
246 showed that the percentage of phase-bright spores gradually increased with
247 elevating the expression level of *ald* (Figure 6A-6C). Notably, the expression of
248 *ald* exhibited a decrease when the concentration of added IPTG increased to1
249 mM, which was possibly due to the toxicity of IPTG to cells (Figure 6C). In
250 contrast, the opposite trend was observed for environmental L-alanine
251 concentration of Δ*ald* mutant, which reached to 3397.4 μM without IPTG
252 induction, while decreased to wild-type levels of 145.9 μM when > 200 μM IPTG
253 was added to elevate the expression of *ald* (Figure 6B). Consequently, Ald-
254 mediated alanine metabolism was responsible for controlling the L-alanine
255 content in the external environment of spores to prevent premature germination,
256 and thus ensuring proper sporulation.
257
258 **RocG regulates both the σ^K-dependent spore release and spore**

259 **properties by providing energy sources**

260

261 As indicated above, RocG-mediated glutamate metabolism regulated both
262 sporulation efficiency and spore quality likely by energy supporting. To further
263 investigate this, we first explored the specific sporulation stage interrupted by
264 *rocG* deletion. To this end, we constructed the fusion of *gfp* to the promotor of
265 sporulation stage-specific sigma factors, σ^F, σ^E, σ^G, and σ^K, which regulate
266 polar division, engulfment, spore maturation and spore release, respectively (6,
267 10, 22, 23). In general, the activation of the specific σ factor can be reflected by
268 the σ-dependent GFP fluorescence, thus visually displaying the impaired
269 sporulation stage (22). Results showed that the activation of σ^F and σ^E in Δ*rocG*
270 mutant were similar with that in wild-type (Figure 7A-7B). As for σ^G, its activation
271 can be achieved in Δ*rocG* mutant although the activation time was delayed
272 (Figure 7C). Notably, although the σ^K-dependent GFP fluorescence in Δ*rocG*
273 mutant appeared properly at t_7, it abnormally existed even until t_{25} (Figure 7D).
274 As σ^K is responsible for regulating the cell wall degrading enzymes, leading to
275 mother cell lysis and spore release (24, 25), its fluorescence is supposed to
276 disappear with spore release. The presence of σ^K-dependent GFP fluorescence
277 at the end of sporulation of Δ*rocG* mutant indicated that its σ^K was activated in
278 the mother cell but failed to regulate mother cell lysis, inferring the impaired
279 spore release process in Δ*rocG* mutant (Figure 7E).

280

281 To further understanding the regulating role of RocG in sporulation, *rocG* was
282 artificially expressed in Δ*rocG* mutant under IPTG-inducible promoter. The
283 results showed that the percentage of released spores increased significantly
284 with elevating the expression level of *rocG* (Figure 8A, B). The addition of more
285 than 10 μM IPTG could remarkably improve the percentage of spore release to
286 the wild-type level (Figure 8B). As hypothesized previously, RocG-mediated
287 glutamate metabolism could provide energy sources to drive sporulation
288 proceeding, we then tested the ATP levels in sporulating cells to verify this.

289 Since previous research has demonstrated that the ATP content of mother cells
290 during sporulation is highest at t_1 (14, 26), we examined ATP content at t_1 in
291 Δ*rocG* mutant with different *rocG* expression levels. Accordingly, the level of
292 ATP in Δ*rocG* mutant increased with elevating the *rocG* expression (Figure 8C).
293 Notably, the ATP content of Δ*rocG* mutant with 50 μM IPTG induction was
294 almost double of the wild type (Figure 8C). Then, we wondered if such high
295 level of ATP in sporulating cells could affect the properties of the future spores.
296 To test this, the spores generated under different concentrations of IPTG
297 induction were purified and examined for the germination phenotypes as well
298 as the DPA content and heat resistance. Interestingly, Δ*rocG* spores with 50 μM
299 IPTG induction showed higher germination efficiency but significantly lower
300 DPA content as well as decreased heat resistance than the wild-type spores
301 (Figure 8D, Figure S3). Taken together, the expression of *rocG* can indeed
302 provide energy support for sporulation, at least the spore release regulated by
303 σ^K, thus contributing to the proper sporulation process. However, exceeded
304 expression of *rocG* can accumulate excessive ATP in sporulating cells, which
305 might adversely affect the spore properties.
306
307 **DISCUSSION**
308
309 Sporulation as a typical bacterial differentiation process has been extensively
310 studied for decades, and the morphological events along with the signal
311 transduction for this process are relatively well elucidated (6-10). However, as
312 an energy-consuming process, the sources of energy supply and the underlying
313 regulating mechanism are lack of research. In addition, how the generated
314 spores keep in dormant state during sporulation remains mysterious. Here, we
315 proved that Ald-mediated alanine metabolism decreased the concentration of
316 the typical germinant L-alanine in sporulating environment to a certain level,
317 thus avoiding premature germination and maintaining spore dormancy.
318 Moreover, we also provided evidences supporting that RocG-mediated

glutamate metabolism ensured proper sporulation, especially mother cell lysis, by regulating ATP levels during sporulation. Additionally, excessively high ATP levels during the sporulation process was supposed to adversely affect the properties of the spores produced, including faster germination efficiency, lower DPA content along with decreased heat resistance. Our data revealed that sporulation was a highly orchestrated and exquisite biological process requiring the balance of diverse metabolism pathways, e.g. alanine catabolism to eliminate surrounding germinants, and glutamate metabolism providing appropriate level of energy to ensure both the sporulation completion and high quality of generated spores.

Our finding of alanine catabolism eliminating the germinant L-alanine leads to another open question that which catabolism pathways or biological reactions are responsible for regulating the balance of other germinants during sporulation. Indeed, in *B. cereus* and *B. subtilis* spores, alanine racemases converting the germinant L-alanine to germination inhibitor D-alanine are detected in the coat, thus they can potentially prevent premature germination (27, 28). As for the glutamate metabolism, except for the metabolite ATP, whether other metabolic intermediates are involved in sporulation needs to be further investigated. In fact, the metabolite 2-oxoglutarate can participate in the synthesis of amino acids, nucleotides, and NADH, and thus is able to potentially affect spore formation (29). Finally, since glutamate is a universal amino group donor and commonly exists in all living organisms (30), whether the other spore-forming bacteria also employ glutamate metabolism as the energy sources for sporulation remains an interesting question worth to be further explored.

METHODS

Strains and plasmids

349 *B. subtilis* strains used in this study are listed Table S1. Plasmids construction
350 is listed in Table S2, and primers are described in Table S3. For gene
351 replacement strategy, primer pairs were used to amplify the flanking genomic
352 regions of the corresponding gene. PCR products and the respective antibiotic
353 resistance gene were used for Gibson assembly (NEB, USA) (31). The product
354 was used to transform *B. subtilis* PY79 to obtain the mutant allele.
355
356 **General methods**
357
358 Sporulation of *B. subtilis* was carried out at 37°C by suspending cells in
359 Schaeffer's liquid medium (Difco Sporulation Medium, DSM) (32). Sporulation
360 t_0 was identified as the third hour after spores suspending in DSM. The
361 percentage of sporulation was evaluated by calculating the ratio of total number
362 of colonies forming units (CFU) before and after heat treatment (80°C, 20 min)
363 (33). The percentage of phase-bright or released spores were counted based
364 on the according phase-contrast images. To ensure confidence of the data, at
365 least 800 cells were counted for each experiment. Spore germination with
366 different germinants was examined as described previously with some
367 modification (14, 34). Briefly, purified spores were heat activated at 75°C for 30
368 min, and then induced by L-Ala (10 mM) or AGFK (2.5 mM L-Asparagine, 5
369 mg/mL D-glucose, 5 mg/mL D-fructose, and 50 mM KCl) at 37°C, by DDA (1
370 mM in 10 mM Tris-HCl, pH 7.4) at 42°C. The germination was tested by
371 determining the DPA release as descried in the following text.
372
373 **Spore purification**
374
375 Matured spores were purified as described previously (14). Briefly, 22 hrs DSM
376 culture was centrifuged and washed 3 times by DDW and then kept in 4°C with
377 constant agitation. The suspension was washed once a day and resuspended
378 in DDW. After 7 days, the suspension was centrifuged to collect the pellet. 20%

379 histodenz solution was used to resuspend the pellet at a ratio of 400 μL per 10
380 mL of DSM for 30 min on ice. Aliquots (200 μL) of resuspension mixture were
381 then added on top of 900 μL 50% histodenz solution, and gradient fractionation
382 was carried out by centrifugation at 15,000 rpm at 4°C for 30 min. The pellet
383 was collected and washed at least 5 times by DDW. Phase contrast microscopy
384 was then used to evaluate the purity of pellet spores. Spores with >99% purity
385 can be used for following experiments, otherwise the purification steps should
386 be carried out more than once.
387
388 **Tandem Mass Tag-based (TMT) quantitative proteomics analysis**
389
390 TMT quantitative proteomics analysis was carried out between pure dormant
391 spores (DS) and vegetative cells (VC) at sporulation t_0 by APTBIO (Shanghai,
392 China). DS and VC samples were collected by centrifugation and then freeze-
393 dried and bead-grinded using FastPrep-24 (M. P. Biomedicals, LLC, USA).
394 Samples were then extracted for proteins and performed the proteomics
395 analysis by LC-MS/MS system. A statistical analysis was performed using a t-
396 test to determine the significance (p-value) of differentially-expressed proteins.
397 The expression level of proteins with $p < 0.05$ and fold change > 1.2 (the
398 expression level increased by more than 1.2-fold or decreased by less than
399 0.83-fold) were considered as significant difference.
400
401 **DPA measurements**
402
403 DPA release was detected as described previously with some modifications
404 (35). Briefly, spore germination was induced by L-Ala, AGFK or DDA at 37°C or
405 42°C in a 96-well plate. Spores (OD_{600} of 10), 10 mM germinants, 25 mM K-
406 Hepes buffer (pH 7.4) as well as 50 mM $TbCl_3$ were mixed in 200 μL and Tb^{3+}-
407 DPA fluorescence intensity was monitored at Ex/Em = 270/545 nm by a TECAN
408 Spark 10M microplate reader (TECAN, Switzerland). Total DPA content of

409 spores were evaluated by boiling the spores (OD_{600} of 1) for 20 min and mixing
410 the spores and 50 mM $TbCl_3$ to 200 μL in a 96-well plate. The DPA standard
411 solution was serially diluted and detected together to obtain a standard curve.
412 The detection parameters for DPA release were the same as above, and the
413 total DPA content of spores was calculated based on the standard curve.
414
415 **Phase-contrast and fluorescence microscopy**
416
417 Phase-contrast and fluorescence microscopy were performed using a Nikon
418 DS-Qi2 microscope equipped with a Nikon Ph3 DL 100x/1.25 Oil phase contrast
419 objective. Both bacterial cells (500 μL) and spores (50 μL) were centrifuged,
420 and the pellets were resuspended with 5 ~ 10 μL PBSx1 and then imaged on
421 the pad. For fluorescence imaging, 1,000 ms exposure time was required for
422 GFP. For time-lapse imaging of sporulation, Imaging System Cell Chamber
423 (AttofluorTM Cell Chamber) was used. Sporulating cells were collected at the
424 late sporulation stage by centrifugation and imaged on a DSM gel-pad with 1%
425 agarose at 37°C. Image analysis and processing were performed by ImageJ2.
426
427 **Real-Time Quantitative PCR (RT-qPCR)**
428
429 Real-time quantitative PCR (RT-qPCR) was carried out followed the protocol
430 described previously (14). RNA samples of sporulating cells (500 μL) were
431 collected from DSM by centrifugation, and then extracted by FastPure
432 Cell/Tissue Total RNA Isolation Kit V2 (Vazyme Biotech Co..Ltd). HiScript III All
433 in-one RT SuperMix for qPCR (Vazyme Biotech Co..Ltd) was used to reverse
434 transcribed RNA samples. RT-qPCR reactions were conducted with
435 PerfectStart Green qPCR SuperMix (TransGen Biotech Co., Ltd). CFX Connect
436 RealTime PCR Dection System (Bio-Rad) was used to detect the fluorescence
437 and *scr* gene that has unchangeable expression level during sporulation was
438 selected to normalize sample data. Each sample was detected in triplicate and

439 at least three independent measurements were conducted.

440

441 **Environmental L-alanine content assay**

442

443 Measurement of environmental L-Alanine level was performed as the
444 instruction of Amplite Fluorimetric L-Alanine Assay Kit (AAT Bioquest, Inc.).
445 DSM media of sporulating cells at indicated timepoints was collected from the
446 supernatant after centrifugation. The fluorescence intensity of L-Alanine in DSM
447 media was monitored by TECAN Spark 10M microplate reader (TECAN,
448 Switzerland) at Ex/Em = 540/590 nm. The standard solution of L-alanine was
449 serially diluted and detected together to obtain a standard curve, and the L-
450 Alanine content in the environment was calculated based on the standard curve.

451

452 **ATP content assay**

453

454 Measurement of ATP content in mother cell was performed using the BacTiter-
455 Glo Microbial Cell Viability Assay (Promega). As guided by the instructions,
456 sporulating cells in DSM at t_1 were collected and detected luminescence using
457 a TECAN Spark 10M microplate reader (TECAN, Switzerland). The standard
458 solution of ATP was serially diluted and detected together to obtain a standard
459 curve and the ATP level was calculated based on the standard curve.

460

461 **Data processing**

462

463 Unless stated otherwise, each experiment was carried out at least three times.
464 GraphPad Prism 8 software was used for all statistical analysis, data
465 processing, and graph drawing. One-way ANOVA was performed to analyze
466 the variance and $p < 0.05$ was regarded as significance for all data statistics.

467

ACKNOWLEDGEMENTS

We are grateful to Dr. Bing Zhou (The Hebrew University of Jerusalem) for valuable discussions and comments. This work was supported by National Natural Science Foundation of China (NSFC) (grant No. 32372470), NSFC (grant No. 32001658), Agricultural Research Outstanding Talents of China (grant No. 13210317) awarded to Lei Rao, and 2115 Talent Development Program of China Agricultural University. The authors declare no conflicts of interest.

REFERENCES

(1) Driks A. 2002. Maximum shields: the assembly and function of the bacterial spore coat. *Trends Microbiol.* 10:251-254.

(2) Stragier P. Losick R. 1996. Molecular genetics of sporulation in *Bacillus subtilis*. *Annu. Rev. Genet.* 30:297-241.

(3) Nicholson W L, Munakata N, Horneck G, Melosh H J. Setlow P. 2000. Resistance of *Bacillus* endospores to extreme terrestrial and extraterrestrial environments. *Microbiol. Mol. Biol. Rev.* 64:548-572.

(4) Setlow P. 2006. Spores of *Bacillus subtilis*: their resistance to and killing by radiation, heat and chemicals. *J. Appl. Microbiol.* 101:514-525.

(5) Vreeland R H, Rosenzweig W D. Powers D W. 2000. Isolation of a 250 million-year-old halotolerant bacterium from a primary salt crystal. *Nature* 407:897-900.

(6) Riley E P, Schwarz C, Derman A I. Lopez-Garrido J. 2020. Milestones in *Bacillus subtilis* sporulation research. *Microb Cell* 8:1-16.

(7) Tokuyasu K. Yamada E. 1959. Fine Structure of *Bacillus subtilis*: II. Sporulation Progress. *The Journal of Cell Biology* 5:129-133.

(8) Kawata T, Inoue T. Takagi A. 1963. Electron microscopy of spore formation and germination in *Bacillus subtilis*. *Jpn. J. Microbiol.* 7:23-41.

(9) Piggot P. Coote J. 1976. Genetic aspects of bacterial endospore formation. *Bacteriol. Rev.* 40:908-962.

(10) Errington J. 2003. Regulation of endospore formation in *Bacillus subtilis*. *Nat. Rev. Microbiol.* 1:117-126.

(11) Phillips Z. Strauch M. 2002. *Bacillus subtilis* sporulation and stationary phase gene expression. *Cell. Mol. Life Sci.* 59:392-402.

(12) Charba J. Nakata H. 1977. Role of glutamate in the sporogenesis of *Bacillus cereus*. *J. Bacteriol.* 130:242-248.

(13) Siranosian K J, Ireton K. Grossman A D. 1993. Alanine dehydrogenase (ald) is required for normal sporulation in *Bacillus subtilis*. *J. Bacteriol.*

508 175:6789-6796.
509 (14) Rao L, Zhou B, Serruya R, Moussaieff A, Sinai L. Ben-Yehuda S.
510 2022. Glutamate catabolism during sporulation determines the success of the
511 future spore germination. *iScience* 25:105242.
512 (15) Driks A. 2002. Overview: development in bacteria: spore formation in
513 *Bacillus subtilis*. *Cell. Mol. Life Sci.* 59:389-391.
514 (16) Ramírez‐Guadiana F H, Meeske A J, Wang X, Rodrigues C D.
515 Rudner D Z. 2017. The *Bacillus subtilis* germinant receptor GerA triggers
516 premature germination in response to morphological defects during sporulation.
517 *Mol. Microbiol.* 105:689-704.
518 (17) Gao Y, Barajas-Ornelas R D C, Amon J D, Ramírez-Guadiana F H,
519 Alon A, Brock K P, Marks D S, Kruse A C. Rudner D Z. 2022. The SpoVA
520 membrane complex is required for dipicolinic acid import during sporulation and
521 export during germination. *Genes Dev.* 36:634-646.
522 (18) Belitsky B R. Sonenshein A L. 1998. Role and regulation of *Bacillus subtilis*
523 glutamate dehydrogenase genes. *J. Bacteriol.* 180:6298-6305.
524 (19) Yoshida K, Fujita Y. Ehrlich S D. 1999. Three asparagine synthetase
525 genes of *Bacillus subtilis*. *J. Bacteriol.* 181:6081-6091.
526 (20) de Vries Y P, Atmadja R D, Hornstra L M, de Vos W M. Abee T. 2005.
527 Influence of glutamate on growth, sporulation, and spore properties of *Bacillus*
528 *cereus* ATCC 14579 in defined medium. *Appl. Environ. Microbiol.* 71:3248-3254.
529 (21) Lin T H, Wei G T, Su C C. Shaw G C. 2012. AdeR, a PucR-type
530 transcription factor, activates expression of L-alanine dehydrogenase and is
531 required for sporulation of *Bacillus subtilis*. *J. Bacteriol.* 194:4995-5001.
532 (22) Meeske A J, Rodrigues C D, Brady J, Lim H C, Bernhardt T G.
533 Rudner D Z. 2016. High-throughput genetic screens identify a large and diverse
534 collection of new sporulation genes in *Bacillus subtilis*. *PLoS Biol.* 14:e1002341.
535 (23) Hilbert D W. Piggot P J. 2004. Compartmentalization of gene expression
536 during *Bacillus subtilis* spore formation. *Microbiol. Mol. Biol. Rev.* 68:234-262.
537 (24) Nugroho F A, Yamamoto H, Kobayashi Y. Sekiguchi J. 1999.

538 Characterization of a new sigma-K-dependent peptidoglycan hydrolase gene
539 that plays a role in *Bacillus subtilis* mother cell lysis. *J. Bacteriol.* 181:6230-
540 6237.
541 (25) Smith T J. Foster S J. 1995. Characterization of the involvement of two
542 compensatory autolysins in mother cell lysis during sporulation of *Bacillus*
543 *subtilis* 168. *J. Bacteriol.* 177:3855-3862.
544 (26) Updegrove T B, Harke J, Anantharaman V, Yang J, Gopalan N,
545 Wu D, Piszczek G, Stevenson D M, Amador-Noguez D. Wang J D. 2021.
546 Reformulation of an extant ATPase active site to mimic ancestral GTPase
547 activity reveals a nucleotide base requirement for function. *elife* 10:e65845.
548 (27) Stewart B T. Halvorson H O. 1953. Studies on the spores of aerobic
549 bacteria I: the occurrence of alanine racemase. *J. Bacteriol.* 65:160-166.
550 (28) Yasuda Y, Kanda K, Nishioka S, Tanimoto Y, Kato C, Saito A,
551 Fukuchi S, Nakanishi Y. Tochikubo K. 1993. Regulation of L-alanine-initiated
552 germination of *Bacillus subtilis* spores by alanine racemase. *Amino Acids* 4:89-
553 99.
554 (29) Huergo L F. Dixon R. 2015. The emergence of 2-oxoglutarate as a master
555 regulator metabolite. *Microbiol. Mol. Biol. Rev.* 79:419-435.
556 (30) Gundlach J, Commichau F M. Stülke J. 2018. Perspective of ions and
557 messengers: an intricate link between potassium, glutamate, and cyclic di-AMP.
558 *Curr. Genet.* 64:191-195.
559 (31) Guérout-Fleury A-M, Frandsen N. Stragier P. 1996. Plasmids for ectopic
560 integration in *Bacillus subtilis*. *Gene* 180:57-61.
561 (32) Harwood C R. Cutting S M. *Molecular biological methods for Bacillus*;
562 Chichester ; New York : Wiley, 1990.
563 (33) Zhou B, Semanjski M, Orlovetskie N, Bhattacharya S, Alon S,
564 Argaman L, Jarrous N, Zhang Y, Macek B, Sinai L. Ben-Yehuda S. 2019.
565 Arginine dephosphorylation propels spore germination in bacteria. *Proc. Natl.*
566 *Acad. Sci. USA* 116:14228-14237.
567 (34) Vepachedu V R. Setlow P. 2007. Role of SpoVA proteins in release of

568 dipicolinic acid during germination of *Bacillus subtilis* spores triggered by
569 dodecylamine or lysozyme. *J. Bacteriol.* 189:1565-1572.
570 (35) Yi X. Setlow P. 2010. Studies of the commitment step in the germination of
571 spores of *Bacillus* species. *J. Bacteriol.* 192:3424-3433.
572

573 **Figure legends**

574

575 **Figure 1.** TMT quantitative proteomic analysis. (A) Proteins were compared
576 between dormant spores (DS) and vegetative cells (VC) of at the onset of
577 sporulation (T_0); (B) Heatmap of differential expression of proteins in DS
578 samples were grouped using Hierarchical Cluster Analysis. Each line
579 represented a protein, with FC > 1.2 and $p < 0.05$ (T-test) as the screening
580 criteria. The proteins with significantly decreased expression were marked in
581 blue, the proteins with significantly increased expression were in red, the
582 proteins without quantitative information were in gray; (C) The volcano map of
583 proteins in DS group was drawn based on two factors of fold change (FC) of
584 differential expression and the P value of T test. The proteins with significantly
585 decreased expression (FC < 0.83, $p < 0.05$) were marked in blue, the proteins
586 with significantly increased expression (FC > 1.2, $p < 0.05$) were in red, and the
587 non-differentiated proteins were in gray; (D) The enrichment map (Top 20) of
588 KEGG pathway enrichment analysis of differentially expressed proteins in the
589 DS group by Fisher's exact test. The color of the bubble represents the
590 significance of the enriched KEGG pathway, and the color gradient represents
591 the size of the P-value (-log10), and the closer to red, the smaller the P-value.
592 The size of the bubble represents the amount of differential protein.

593

594 **Figure 2.** Alanine and glutamate metabolism co-regulate sporulation with an
595 additive effect. (A) Phase-contrast images of sporulating cells at the late
596 sporulation stage t_{19}. *B. subtilis* PY79 (wt), YZ11 (Δ*ald*), YZ19 (Δ*rocG*), YZ12
597 (Δ*ald* Δ*rocG*) and YZ13 (Δ*ald* Δ*rocG*, *amyE::ald-rocG*) strains were induced to
598 sporulate in DSM at 37°C for 22 hrs and followed by microscopy. Images
599 captured from a representative experiment out of three independent biological
600 repeats. Scale bar, 2 μm; (B) The percentage of sporulation of the strains
601 described in (A). Data are presented as the percentage of total number of
602 colonies forming units (CFU) before and after heat treatment (80°C, 20 min).

603 Shown are average values and SD obtained from three independent biological
604 repeats.
605
606 **Figure 3.** RocG-mediated glutamate metabolism is essential for ensuring the
607 sporulation efficiency. (A) Phase-contrast images of sporulating cells at the late
608 sporulation stage t_{19}. *B. subtilis* PY79 (wt), YZ22 (Δ*ald* Δ*rocG* Δ*gerAA*), YZ24
609 (Δ*ald* Δ*rocG* Δ*gerAA, amyE::P*$_{IPTG}$*-rocG*), YZ25 (Δ*ald* Δ*rocG* Δ*gerAA,*
610 *amyE::P*$_{IPTG}$*-ald*) and YZ26 (Δ*ald* Δ*rocG* Δ*gerAA, amyE::P*$_{IPTG}$*-rocG-ald*) strains
611 were induced to sporulate in DSM at 37°C for 22 hrs and followed by
612 microscopy. 50 μM IPTG was added to the YZ24, YZ25 and YZ26 cultures at
613 the sporulation t_0 to induce corresponding gene expression. Images captured
614 from a representative experiment out of three independent biological repeats.
615 Scale bar, 2 μm; (B) Quantification of the experiment described in (A). Data are
616 presented as percentages of the number of the phase-bright spores and all
617 sporulating cells in the same image. Shown are average values and SD
618 obtained from three independent biological repeats (n ≥ 800 for each strain);
619 (C) Spores of wt, as well as YZ24, YZ25 and YZ26 strains with 50 μM IPTG
620 induction, were incubated with AGFK (10 mM) to trigger germination. DPA
621 release was measured by detecting the relative fluorescence units (RFU) of
622 Tb^{3+}-DPA. Shown is a representative experiment out of three independent
623 biological repeats.
624
625 **Figure 4.** The expression of *rocG* is significant to the quality of correspondingly
626 generated spores. (A) Phase-contrast images of sporulating cells at the late
627 sporulation stage t19. *B. subtilis* PY79 (wt), YZ81 (Δ*adeR* Δ*gerAA*), YZ23
628 (Δ*ahrC* Δ*rocR* Δ*gerAA*) and YZ90 (Δ*adeR* Δ*ahrC* Δ*rocR* Δ*gerAA*) strains were
629 induced to sporulate in DSM at 37°C for 22 hrs and followed by microscopy.
630 Images captured from a representative experiment out of three independent
631 biological repeats. Scale bar, 2 μm; (B) Expression of the *ald* gene in wt, YZ11

632 (Δ*ald*) and YZ81 strains, and *rocG* gene in wt, YZ19 (Δ*rocG*) and YZ23 strains;
633 (C) Spores of wt, YZ81, YZ23 and YZ90 strains were incubated with AGFK (10
634 mM) to trigger germination. DPA release was measured by detecting the
635 relative fluorescence units (RFU) of Tb^{3+}-DPA. Shown is a representative
636 experiment out of three independent biological repeats.
637
638 **Figure 5.** The absence of Ald induces premature germination during sporulation.
639 (A) Phase-contrast images of sporulating cells at the late sporulation stage t_{19}.
640 *B. subtilis* PY79 (wt), YZ11 (Δ*ald*) and YZ21 (Δ*ald* Δ*gerAA*) strains were
641 induced to sporulate in DSM at 37°C for 22 hrs and followed by microscopy.
642 Images captured from a representative experiment out of three independent
643 biological repeats. Scale bar, 2 μm; (B) Quantification of the experiment
644 described in (A). Data are presented as percentages of the number of the
645 phase-bright spores and all sporulating cells in the same image. Shown are
646 average values and SD obtained from three independent biological repeats (n
647 ≥ 800 for each strain); (C) Spores of wt, YZ11 and YZ21 strains were incubated
648 with AGFK (10 mM) to trigger germination. DPA release was measured by
649 detecting the relative fluorescence units (RFU) of Tb^{3+}-DPA. Shown is a
650 representative experiment out of three independent biological repeats. (D)
651 Models of the premature germination in Δ*ald* mutant. YZ11 strain was induced
652 to sporulate in DSM at 37°C. After 14 hrs of incubation, spores were collected
653 on a DSM gel-pad, and followed by time-lapse microscopy at a 10 min interval.
654
655 **Figure 6.** Ald-mediated alanine metabolism regulates L-alanine content in the
656 external environment of spores. (A) Phase-contrast images of sporulating cells
657 at the late sporulation stage t_{19}. YZ31 (Δ*ald, amyE::P*$_{IPTG}$*-ald*) strains were
658 induced to sporulate in DSM at 37°C for 22 hrs and followed by microscopy. 0-
659 1000 μM IPTG was added at the sporulation t_0 to induce *ald* expression. Images
660 captured from a representative experiment out of three independent biological
661 repeats. Scale bar, 2 μm; (B) The percentage of phase-bright spores as well as

662 the environmental L-alanine content of the wt and YZ31 strains described in (A).
663 The percentage of phase-bright spores are presented as ratio of the number of
664 the phase-bright spores and all sporulating cells in the same image (n ≥ 800 for
665 each strain). The environmental L-alanine content was evaluated at the end of
666 sporulation; (C) Expression of the *ald* gene in YZ31 strains described in (A).
667 Shown are average values and SD obtained from three independent biological
668 repeats.
669
670 **Figure 7.** Cytological sporulation assay reveals the impaired sporulation stage
671 of Δ*rocG* mutants. (A-D) Phase contrast and the indicated fluorescent images
672 of wt and YZ19 (Δ*rocG*) cells harboring four transcriptional fusions, σ^F, σ^E, σ^G
673 and σ^K, at sporulation t_2, $t_{2.5}$, t_4 and t_{25}, t_7 and t_{25}, respectively. Images captured
674 from a representative experiment out of three independent biological repeats.
675 Scale bar, 2 μm; (E) Models of the sporulation defect in Δ*rocG* mutants.
676
677 **Figure 8.** RocG regulates both spore release and spore properties. (A) Phase-
678 contrast images of sporulating cells at the late sporulation stage t_{19}. *B. subtilis*
679 PY79 (wt), YZ19 (Δ*rocG*) and YZ32 (Δ*rocG, amyE::P*$_{IPTG}$*-rocG*) strains were
680 induced to sporulate in DSM at 37°C for 22 hrs and followed by microscopy. 0-
681 50 μM IPTG was added to YZ32 at the sporulation t_0 to induce *rocG* expression.
682 Images captured from a representative experiment out of three independent
683 biological repeats. Scale bar, 2 μm; (B) Quantification of the experiment
684 described in (A). Data are presented as percentages of the number of the
685 released spores and all sporulating cells in the same image. Shown are
686 average values and SD obtained from three independent biological repeats (n
687 ≥ 800 for each strain); (C) Strains indicated in (A) were grown in DSM
688 sporulation medium. IPTG was added to the YZ32 cultures at the t_0 to induce
689 *rocG* expression. The DSM cultures were collected at t_1 and analyzed for ATP
690 level. Shown are average values and SD obtained from three independent
691 biological repeats. (D) Spores of wt and YZ32 strains with different IPTG

692 induction were incubated with (i) L-alanine (10 mM), (ii) AGFK (10 mM) and (iii)
693 DDA (10 mM) to trigger germination. Total DPA content (iv) of these spores were
694 measured by boiling for 20 min. DPA release was measured by detecting the
695 relative fluorescence units (RFU) of Tb^{3+}-DPA. Shown is a representative
696 experiment out of three independent biological repeats.
697

Figure 1

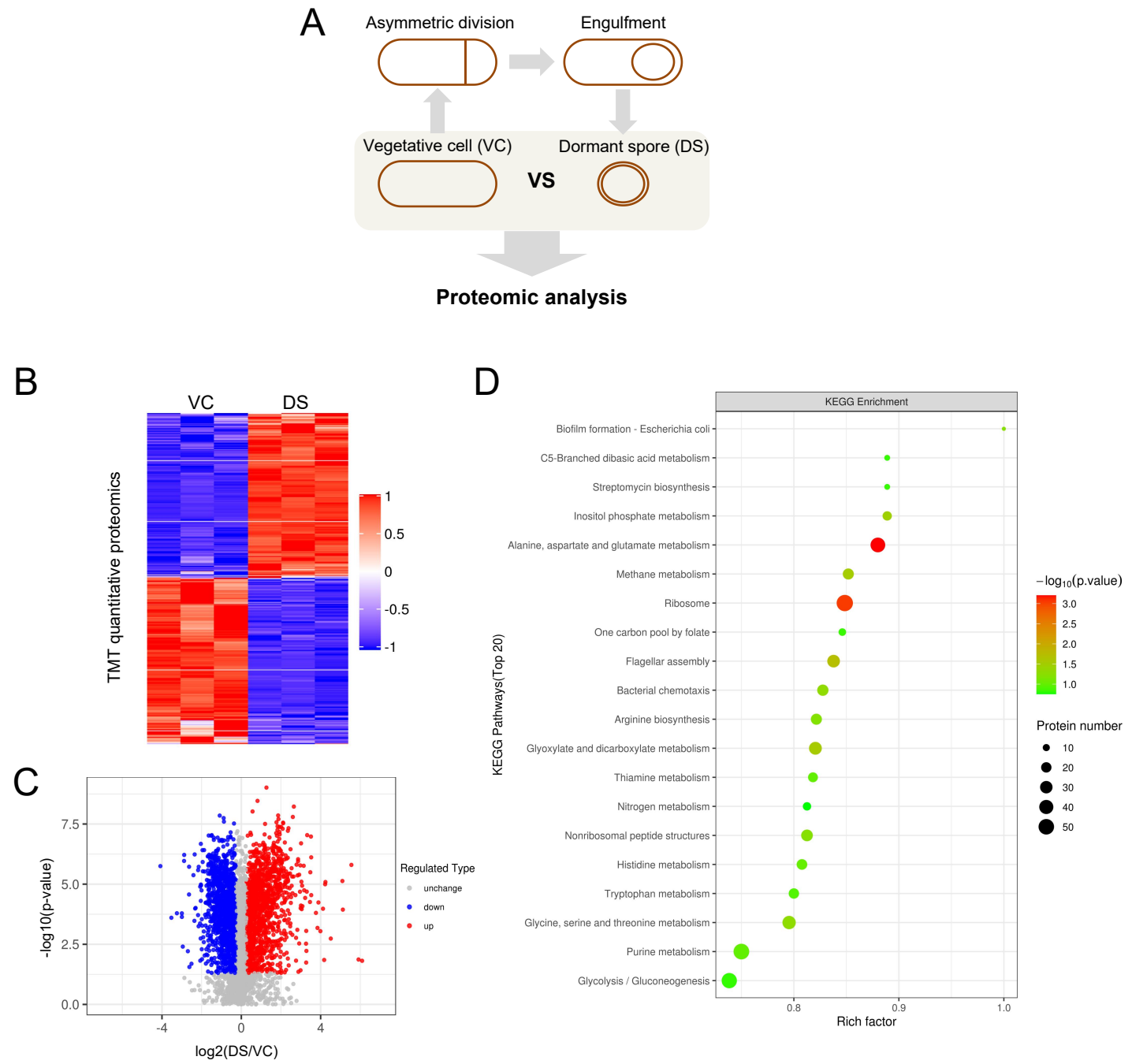
A
Asymmetric division
Engulfment
Vegetative cell (VC)
Dormant spore (DS)
VS
Proteomic analysis
B
VC
DS
TMT quantitative proteomics
1
0.5
0
-0.5
-1
C
-log10(p-value)
log2(DS/VC)
Regulated Type
unchange
down
up
D
KEGG Enrichment
KEGG Pathways(Top 20)
Biofilm formation - Escherichia coli
C5-Branched dibasic acid metabolism
Streptomycin biosynthesis
Inositol phosphate metabolism
Alanine, aspartate and glutamate metabolism
Methane metabolism
Ribosome
One carbon pool by folate
Flagellar assembly
Bacterial chemotaxis
Arginine biosynthesis
Glyoxylate and dicarboxylate metabolism
Thiamine metabolism
Nitrogen metabolism
Nonribosomal peptide structures
Histidine metabolism
Tryptophan metabolism
Glycine, serine and threonine metabolism
Purine metabolism
Glycolysis / Gluconeogenesis
Rich factor
−log10(p.value)
Protein number

Figure 2

A

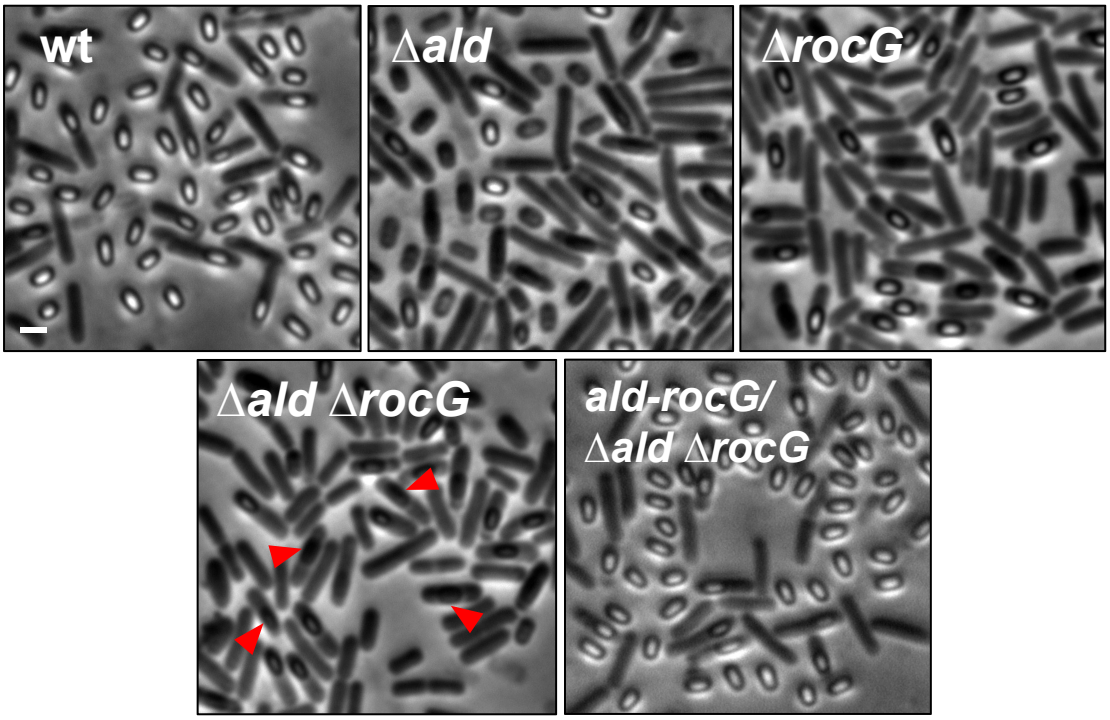
wt
Δald
ΔrocG
Δald ΔrocG
ald-rocG/
Δald ΔrocG

B

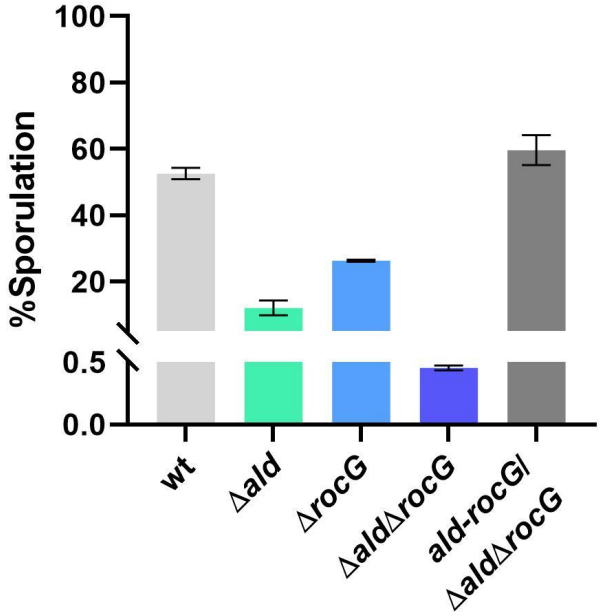
%Sporulation
100
80
60
40
20
0.5
0.0
wt
Δald
ΔrocG
ΔaldΔrocG
ald-rocG/
ΔaldΔrocG

Figure 3

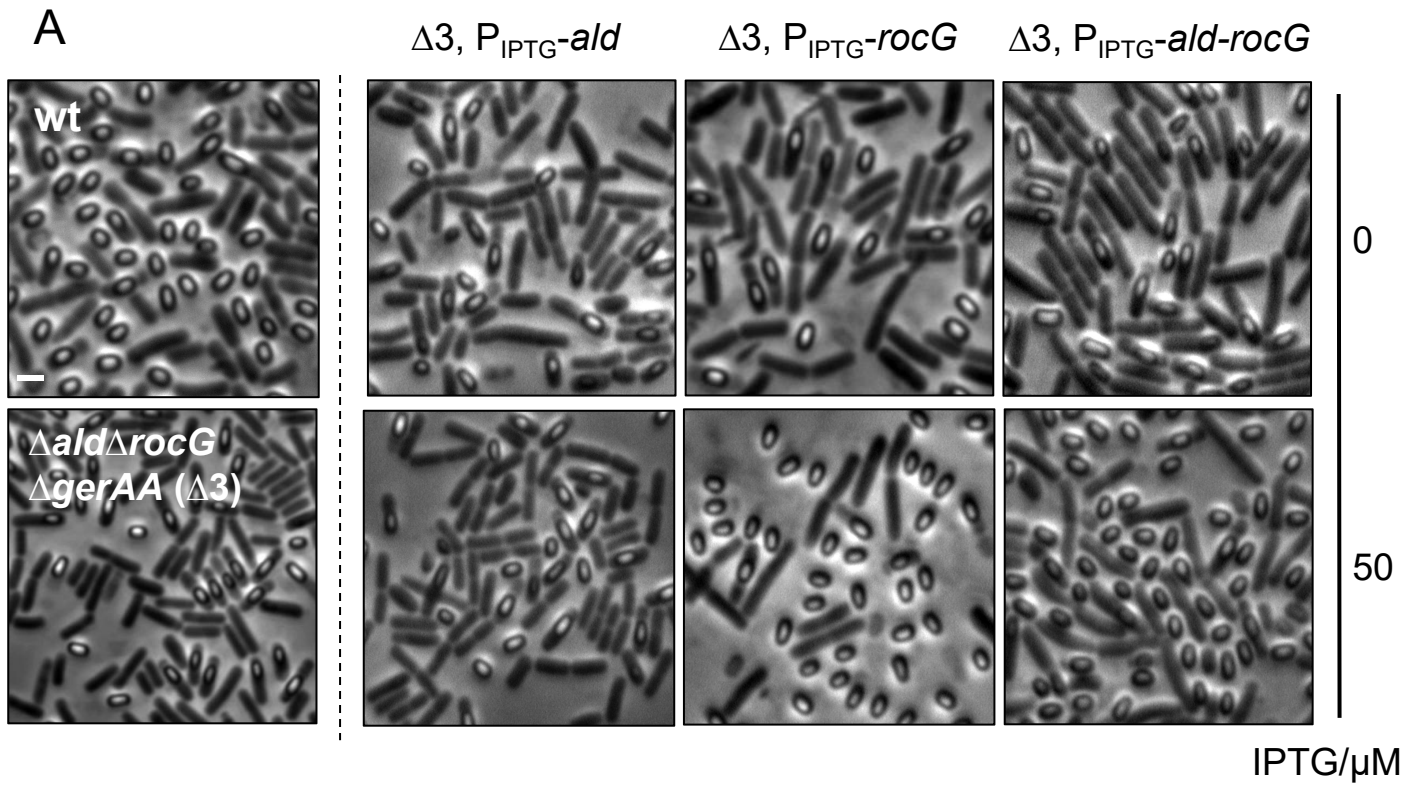
A
Δ3, P_IPTG-ald
Δ3, P_IPTG-rocG
Δ3, P_IPTG-ald-rocG
wt
ΔaldΔrocG
ΔgerAA (Δ3)
0
50
IPTG/μM

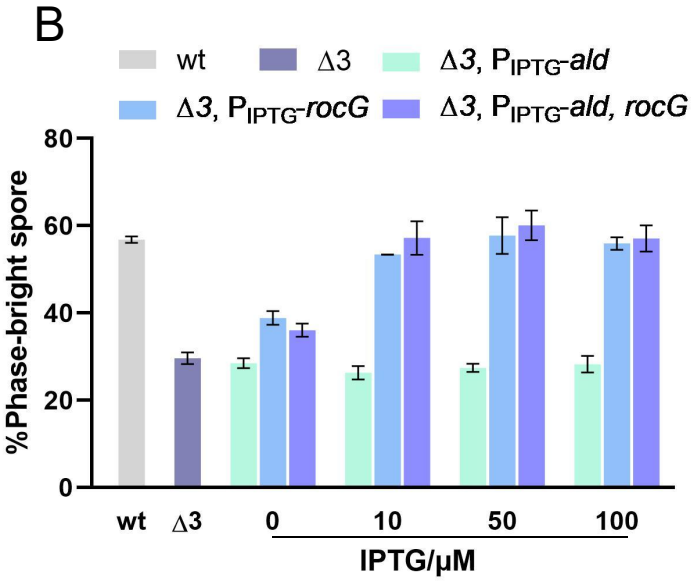
B
wt
Δ3
Δ3, P_IPTG-ald
Δ3, P_IPTG-rocG
Δ3, P_IPTG-ald, rocG
%Phase-bright spore
80
60
40
20
0
wt
Δ3
0
10
50
100
IPTG/μM

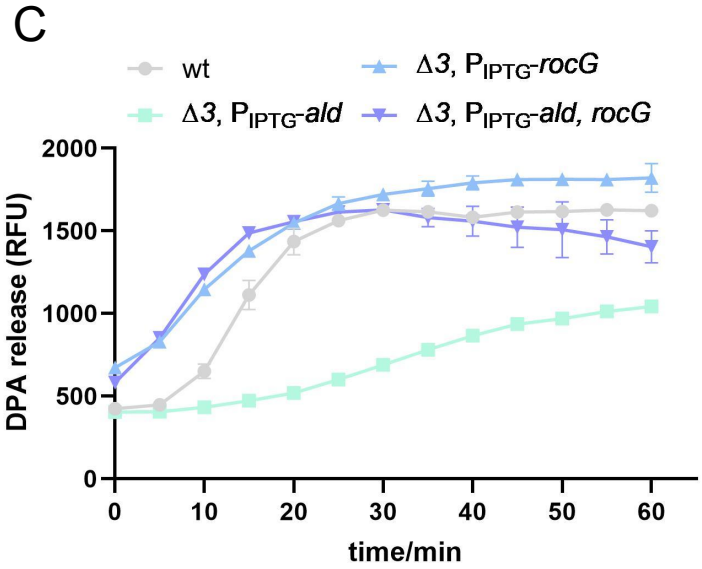
C
wt
Δ3, P_IPTG-rocG
Δ3, P_IPTG-ald
Δ3, P_IPTG-ald, rocG
DPA release (RFU)
2000
1500
1000
500
0
0
10
20
30
40
50
60
time/min

Figure 4

A

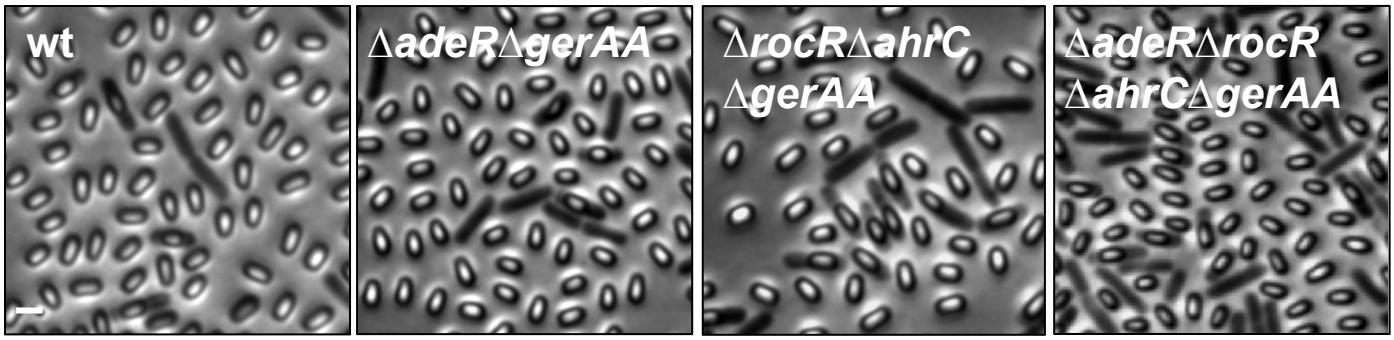
wt
ΔadeRΔgerAA
ΔrocRΔahrC
ΔgerAA
ΔadeRΔrocR
ΔahrCΔgerAA

B

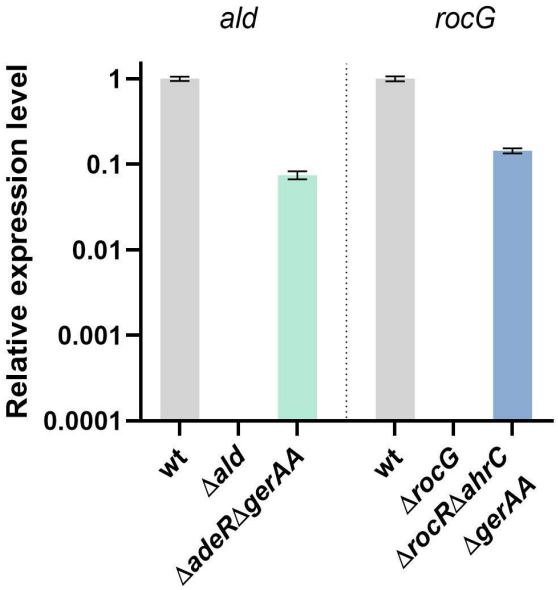
ald
rocG
Relative expression level
1
0.1
0.01
0.001
0.0001
wt
Δald
ΔadeRΔgerAA
wt
ΔrocG
ΔrocRΔahrC
ΔgerAA

C

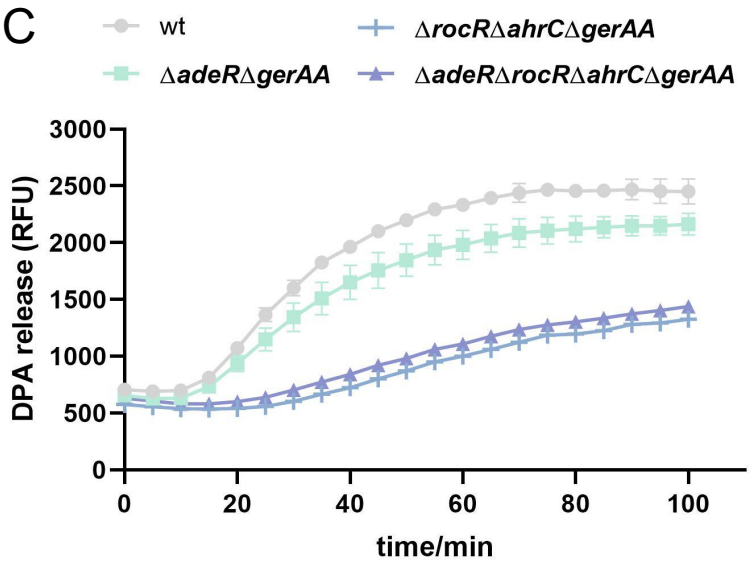
wt
ΔrocRΔahrCΔgerAA
ΔadeRΔgerAA
ΔadeRΔrocRΔahrCΔgerAA
DPA release (RFU)
3000
2500
2000
1500
1000
500
0
0
20
40
60
80
100
time/min

Figure 5

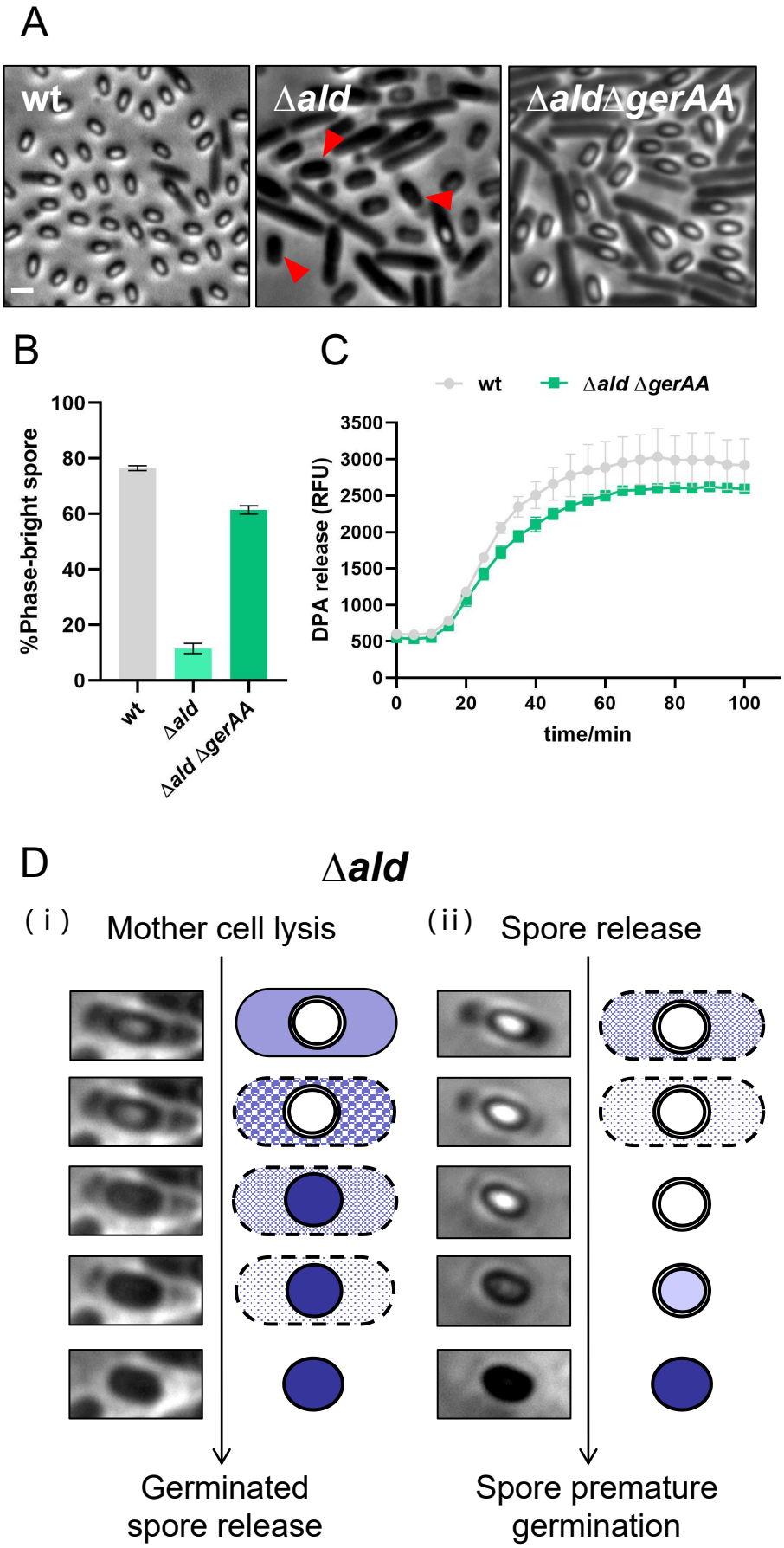
A
wt
Δald
ΔaldΔgerAA
B
%Phase-bright spore
100
80
60
40
20
0
wt
Δald
Δald ΔgerAA
C
wt
Δald ΔgerAA
DPA release (RFU)
3500
3000
2500
2000
1500
1000
500
0
0
20
40
60
80
100
time/min
D
Δald
(i)
Mother cell lysis
(ii)
Spore release
Germinated
spore release
Spore premature
germination

Figure 6

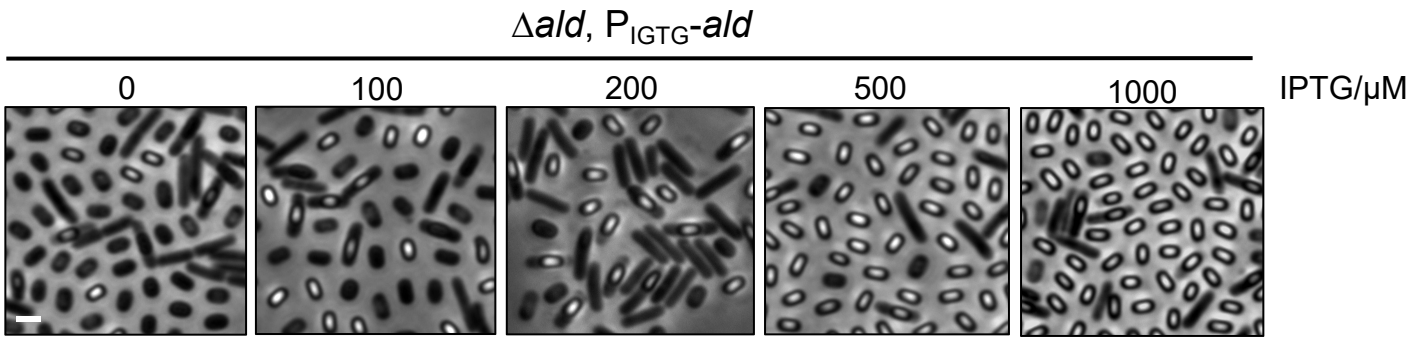
A
Δald, PIGTG-ald
0
100
200
500
1000
IPTG/μM

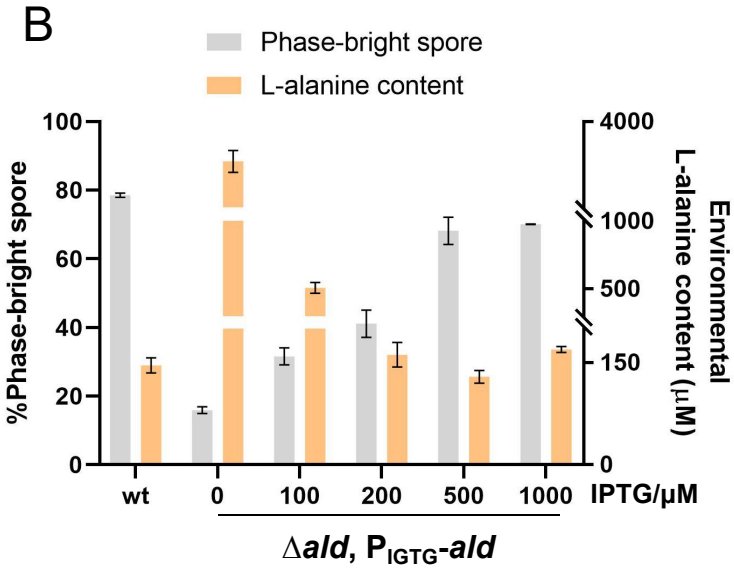
B
Phase-bright spore
L-alanine content
%Phase-bright spore
Environmental L-alanine content (μM)
100
80
60
40
20
0
4000
1000
500
150
0
wt
0
100
200
500
1000
IPTG/μM
Δald, PIGTG-ald

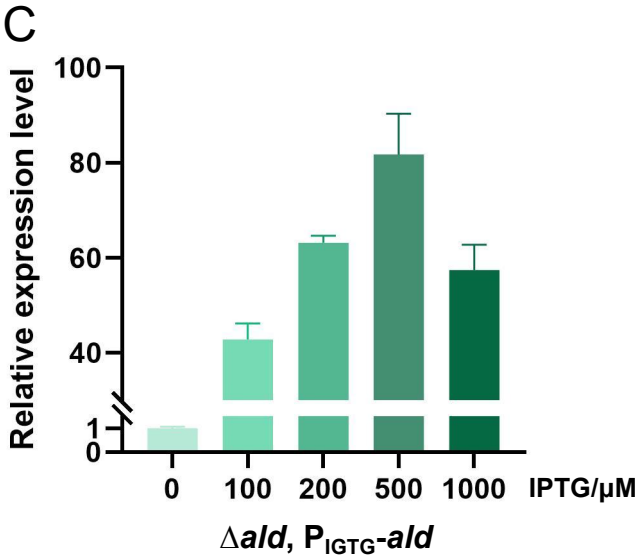
C
Relative expression level
100
80
60
40
1
0
0
100
200
500
1000
IPTG/μM
Δald, PIGTG-ald

Figure 7

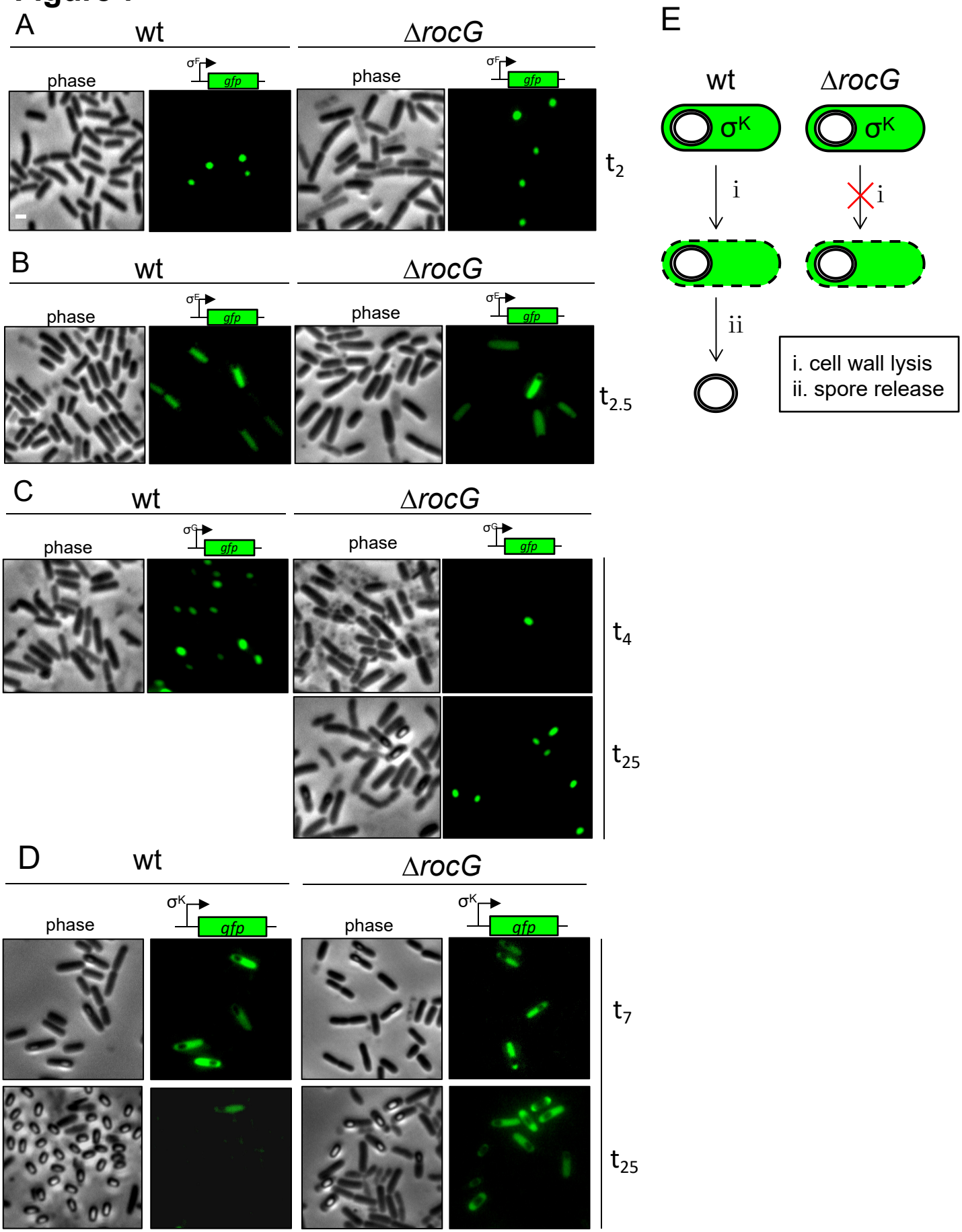
A
wt
ΔrocG
phase
σF
gfp
t2
B
t2.5
C
σG
t4
t25
D
σK
t7
E
i
ii
i. cell wall lysis
ii. spore release

Figure 8

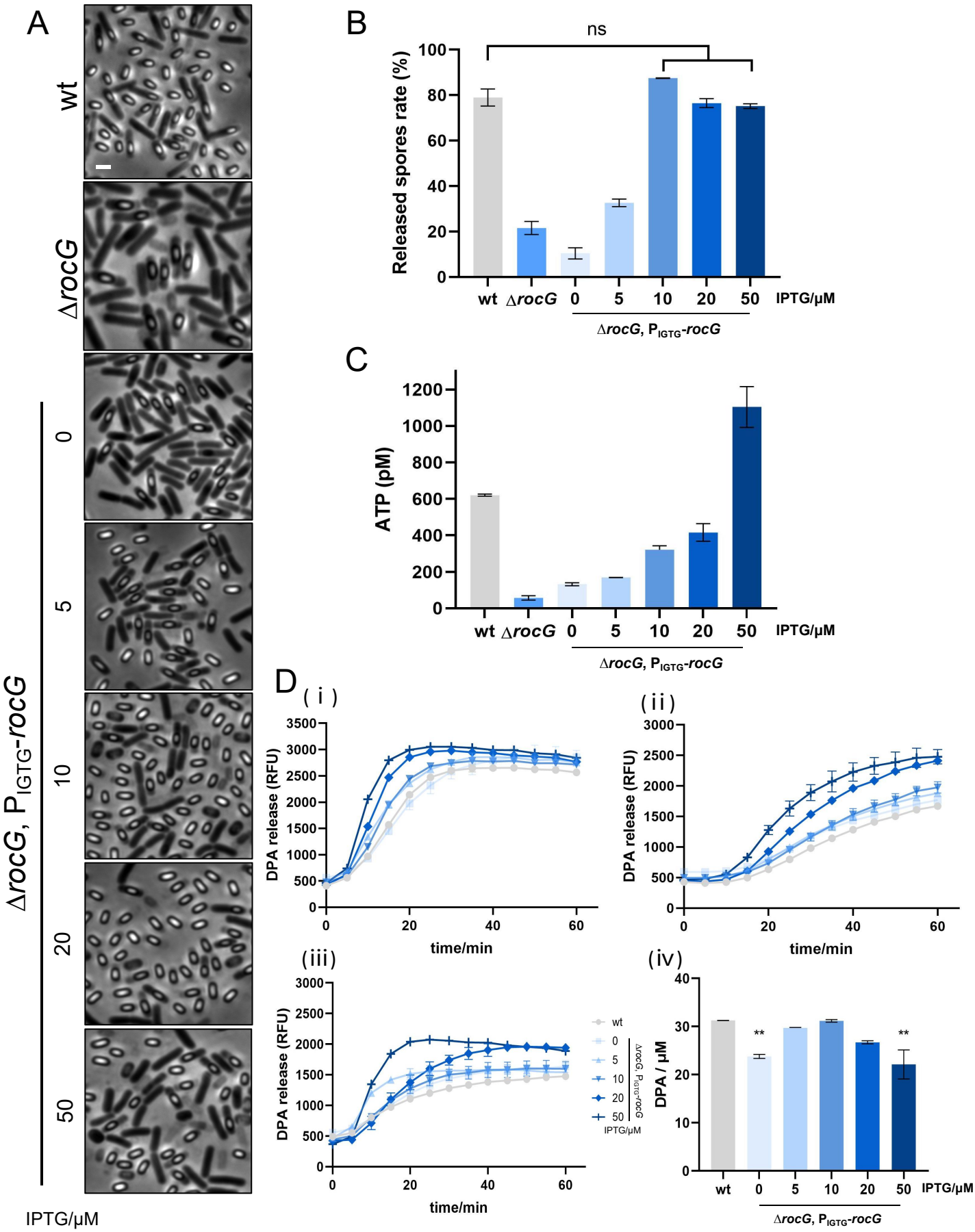
A
wt
ΔrocG
ΔrocG, P_IGTG-rocG
0
5
10
20
50
IPTG/μM
B
ns
Released spores rate (%)
100
80
60
40
20
0
wt
ΔrocG
0
5
10
20
50
IPTG/μM
ΔrocG, P_IGTG-rocG
C
ATP (pM)
1200
1000
800
600
400
200
0
wt
ΔrocG
0
5
10
20
50
IPTG/μM
ΔrocG, P_IGTG-rocG
D
(i)
(ii)
(iii)
(iv)
DPA release (RFU)
time/min
wt
0
5
10
20
50
IPTG/μM
ΔrocG, P_IGTG-rocG
DPA / μM
**
**
wt
0
5
10
20
50
IPTG/μM
ΔrocG, P_IGTG-rocG